Pergamon

Cement and Concrete Research 29 (1999) 159–170

CEMENT AND CONCRETE RESEARCH

Pore solution chemistry of alkali-activated ground granulated blast-furnace slag[1]

Sujin Song [a], Hamlin M. Jennings [a,b,*]

[a]*Department of Materials Science and Engineering, Northwestern University, 2145 Sheridan Road, Evanston, Illinois 60208, USA*
[b]*Department of Civil Engineering, Northwestern University, Evanston, Illinois, USA*

Manuscript received 12 November 1998; accepted manuscript 16 November 1998

Abstract

The chemical composition and pH of the pore solution extracted from six different ground granulated blast-furnace slag (GGBFS) pastes were determined. The concentrations of Si, Ca, Al, and Mg are functions of the pH of the aqueous phase, with high pH associated with the higher concentrations of Si and Al and the lower concentrations of Ca and Mg. When GGBFS is mixed with an aqueous phase with pH higher than 11.5, the reaction is activated or accelerated. The main hydration product was identified as C-S-H, and hydrotalcite, at later stages of hydration, was observed in the pastes with an aqueous phase of a high pH. The effect of pore solution on the alkali activation of GGBFS is discussed with reference to the hydration products. © 1999 Elsevier Science Ltd. All rights reserved.

Keywords: Ground granulated blast-furnace slag; Hydration; pH; Pore solution

Ground granulated blast-furnace slag (GGBFS) is a glassy granular material formed when molten blastfurnace slag is rapidly cooled, usually by immersion in water, and then ground to improve its reactivity. Blast-furnace slag has been used as a pozzolanic admixture in Portland cement paste [1–6]. The major components of blast-furnace slag are SiO_2, CaO, MgO, and Al_2O_3, which are common components in commercial silicate glasses.

Various studies of cementitious materials suggest that the pH of the solution plays an important role in the hydration process and in determining the nature of C-S-H. It was reported that C-S-H does not form in a solution with a pH below 9.5 [7]. Also the formation of C-S-H is dependent on the silicate species in solution, which is affected by pH [8,9]. High [Si] in the aqueous solution comes with low [Ca]. By investigating the solubility of colloidal silica in solutions of electrolytes and in alkaline solutions [10–12], it has been shown that a high pH of the solution produces high [Si].

The effect of pH on the structure and composition of C-S-H, however, is still controversial. Whereas Andersson et al. [13] claim there is no obvious correlation between pH and the chemical compositions of the aqueous solution, others report that the C/S ratio in the pore solution depends on the pH and alkali content of the pore solution; a high C/S ratio is established in solutions of high pH or high alkali content [14–19]. Others have reported that C-S-H gels with low C/S ratios in solutions of high pH or high alkali content [20–24] are associated with solutions of high pH or high alkali content.

Following the general model for the structure and composition of C-S-H gel described by Richardson and Groves [25] and Kersten [26] has shown that C-S-H can be considered a solid solution of tobermorite-like C-S-H ($Ca_2H_2SiO_7 \cdot 3H_2O$) and CH. For this "solid solution-aqueous solution (SSAS)" equilibrium model, the solubility products of the pure endmembers are assumed to compose the solid solution, and they are determined by the following mass action laws:

$$Ca_2H_2SiO_7 \cdot 3H_2O = \{H_3SiO_4^-\}^2 \{CaOH^+\}^2 = K_{CS}^2$$

$$Ca(OH)_2 = \{CaOH^+\} \{OH^-\} = K_{CH}$$

The solubility products were calculated with activities of the monovalent Ca species, $CaOH^+$, as a common cation to give values of $pK_{CH} = 4.0$ and $pK_{CS} = 7.8$, using the thermodynamic database. When K_{CH} is constant, the activity of $CaOH^+$, $\{CaOH^+\}$, must decrease when $\{OH^-\}$ increases, resulting in a higher pH. Likewise, $\{H_3SiO_4^-\}$ must increase with decreasing $\{CaOH^+\}$ because of constant K_{CS}, which explains the low concentration of aqueous silica when the concentration of aqueous Ca species is high [13–24]. When the aqueous solution has a high silica concentra-

* Corresponding author. Tel.: (+1) 847-491-4858; Fax: (+1) 847-467-1078; E-mail: h-jennings@nwu.edu.

[1]This paper was originally submitted to *Advanced Cement Based Materials*. The paper was received at the Editorial Office of *Cement and Concrete Research* on 12 November 1998 and accepted in final form on 16 November 1998.

0008-8846/99/$–see front matter © 1999 Elsevier Science Ltd. All rights reserved.
PII: S0008-8846(98)00212-9

tion, but low calcium, the C-S-H formed in the solution is expected to have a low C/S ratio [27].

There is only scanty information about the chemistry of the pore solution in alkali-activated GGBFS pastes, whereas the pore solution chemistry of ordinary Portland cements (OPC) hydration is fairly well documented. Although slag without an activator does react with water, the rate of hydration is very slow. Its hydraulic reactivity depends on chemical composition, glass phase content, particle size distribution, and surface morphology [1–3]. Mehta [3] reported that a coating of aluminosilicate forms on the surfaces of slag grains within a few minutes of exposure to water, and these coatings were impermeable to water. Unless a chemical activator is present, further hydration is inhibited. Portland cement, gypsum, and many alkalies have been used as activators, and, generally, the rate of hydration is faster at high alkali concentrations. The surface of slag is amorphous, and its dissolving behavior is very similar to that of silicate glasses. Goto et al. [28] found that the solubility of synthetic silica-alumina gel is strongly affected by its composition and the pH of the solution. In this paper, the chemical composition and pH of the pore solutions extracted from six different GGBFS pastes are reported. The effect of pore solution on the alkali activation of GGBFS is discussed with reference to the products formed.

1. Experimental procedure

The chemical composition of the GGBFS used in this study was 37.98% SiO_2, 7.93% Al_2O_3, 39.11% CaO, 11.45% MgO, 0.44% Fe_2O_3, 0.46% TiO_2, 0.31% Na_2O, 0.36% K_2O, and 0.62% MnO. The Blaine fineness was 5565 cm^2/g. The pastes were mixed with de-ionized (DI) water or an NaOH solution of concentrations 1M, 0.4M, and 0.1M using a Hobart mixer for 5 min at the speed setting of 1. The mass ratio of solution to slag (L/S) was 0.45 by weight. The mixes were cast into plastic tubes and sealed before placing the samples in a 25°C water bath.

The extraction of pore fluids was described by Christensen [29] and Christensen et al. [30]. The filtration procedures were performed in a glove box under a nitrogen atmosphere. When the pastes were rigid, pore fluid was extracted using a high-pressure steel die; details are given elsewhere [31]. All the liquid samples were sealed to minimize any carbonation or oxidation of samples and were stored in a nitrogen-filled container. The pH of pore fluids was measured using a digital pH meter, and the concentrations of Si, Al, Ca, and Mg in a pore solution were measured using inductively coupled plasma spectroscopy. X-ray diffraction (XRD) was used to identify the phases present in hydration products. To prepare samples for XRD, pastes were crushed using a mortar and pestle and flushed with acetone, using a porous ceramic filter and vacuum, to stop the hydration at the desired ages. The powder samples were dried in a vacuum. The diffraction conditions were 40 kV, 15 mA, CuKα radiation (λ = 0.1542 nm), 0.05° 2θ step size, and 3 s/step.

In addition to these samples, two samples with different mass ratio of solution to slag also were prepared to produce highly hydrated paste. After slag and DI water were mixed with L/S = 3.0, the paste was placed in an air-tight plastic

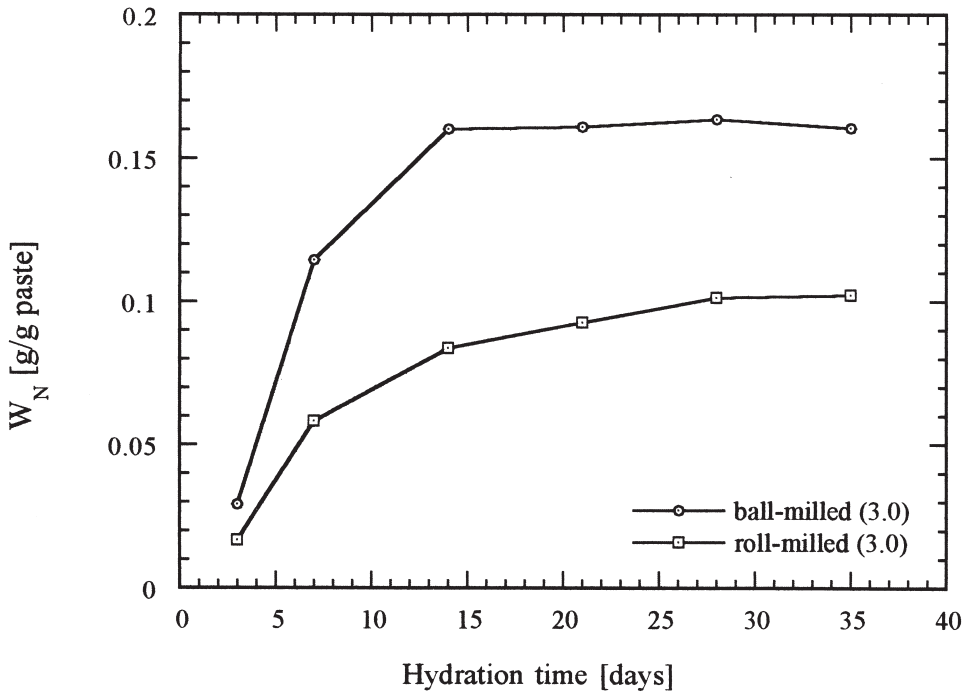

Fig. 1. Loss of ignition of GGBFS pastes mixed with DI water (L/S = 3.0) and continuously milled during the hydration.

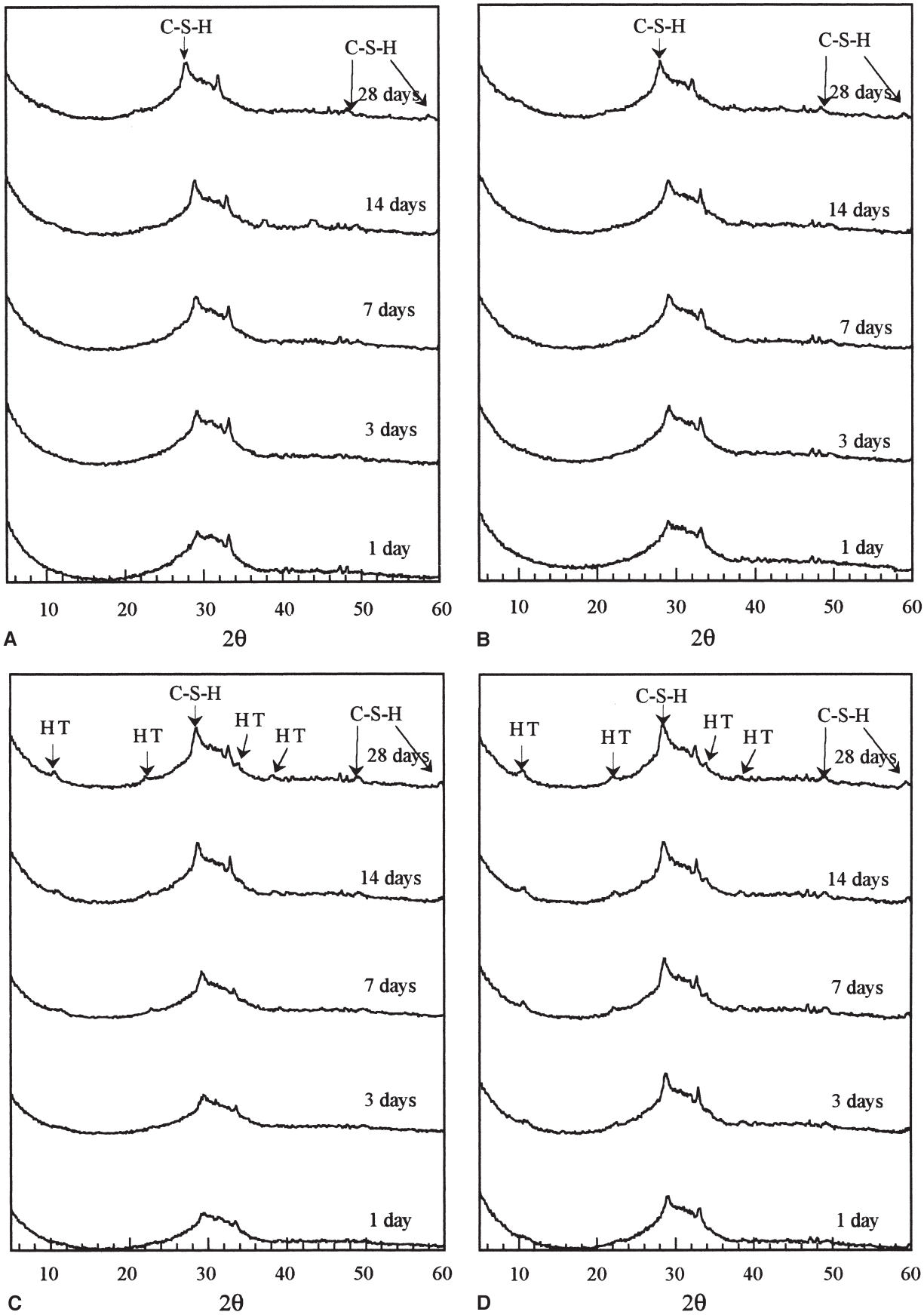

Fig. 2. X-ray diffraction of GGBFS pastes mixed with *(A)* DI water, *(B)* 0.1M, *(C)* 0.5M, and *(D)* 1.0M NaOH solutions. HT, hydrotalcite.

bottle and continuously rolled on the mill for 35 days. Another paste with the same L/S was placed in an airtight plastic bottle and ground continuously on the mill with about 50% volume fraction of stainless steel balls for the same 35 days. Paste samples were removed periodically, and their solid and aqueous phases were analyzed using the same procedure as for the paste with L/S = 0.45.

The nonevaporable water content, W_N, was calculated as the mass difference between the paste dried at 105°C and the same paste after it was ignited at 1005°C. The values were corrected for the loss on ignition of the slag itself, which was measured in a separate experiment. The experimental details are given elsewhere [29]. To determine the degree of hydration, the amount of nonevaporable water in two roll-milled GGBFS pastes are shown as a function of hydration time in Fig. 1. The paste ground with steel balls showed little change in W_N after 14 days of grinding, and the paste without steel balls showed little change in W_N after 28 days. The paste rotated without steel balls has W_N that is only 57% of the W_N of the paste ground with steel balls. The paste roll-milled with stainless steel balls was considered to have reached maximum hydration, and a value of 0.162 g H_2O/g paste was determined at full hydration.

2. Results and discussion

2.1. X-ray diffraction

The accelerated hydration of GGBFS by NaOH was observed using XRD (Fig. 2). The broad and diffuse peak around $2\theta = 30°$ is the result of the short range order of the $CaO\text{-}SiO_2\text{-}Al_2O_3\text{-}MgO$ glass structure from unreacted GGBFS. The peak identified at about $2\theta = 29.5°$ is from the (110) reflection of poorly crystalline C-S-H, which is the main hydration product in all the samples. It should be noted that calcium hydroxide (CH) was not present in any GGBFS pastes, even with a very high water to slag ratio. In the pastes activated with 0.4M and 1M NaOH (Figs. 2C and 2D), additional peaks at $2\theta = 11.6$, 23.0, 34.9, and 39.5 were observed after 3 days of hydration. These correlate with the (003), (006), (012), and (015) reflections of hydrotalcite as given by Gastuche et al. [32]. Hydrotalcite, which is a natural mineral $Mg_6Al_2CO_3(OH)_{16}\cdot 4H_2O$, has been reported in pastes of Portland cement/slag blends [33–36]. The hydrotalcite phase also was observed in blast-furnace slag activated by 5M NaOH using differential thermal analysis and x-ray microanalysis [37], and in GGBFS pastes activated by 5M KOH solution using XRD [33].

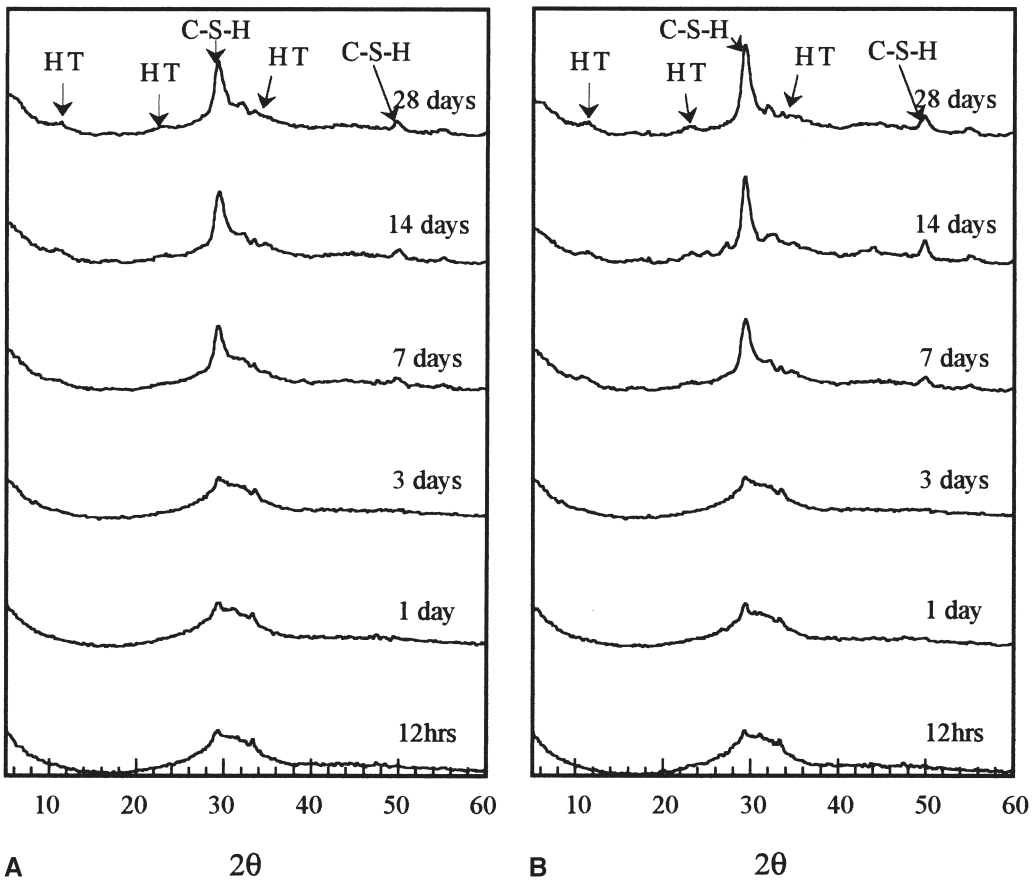

Fig. 3. X-ray diffraction of GGBFS pastes mixed with DI water (L/S = 3.0) and continuously milled during the hydration *(A)* without any grinding media and *(B)* with stainless steel balls as grinding media.

The roll-milled GGBFS pastes with high water to slag ratio (L/S = 3.0) provided an answer to the question as to whether or not hydrotalcite forms only in GGBFS pastes with high alkalis. Because both roll-milled pastes with high water to slag ratio (L/S = 3.0) contained C-S-H and hydrotalcite as well (Fig. 3), hydrotalcite can form in the pastes mixed only with DI water. Hydrotalcite is apparently a phase that forms when a high degree of hydration is reached in GGBFS pastes, and this should be taken into account when the long-term performance of GGBFS pastes is of interest. Because the paste ground with steel balls showed faster hydration than the paste that was simply rotated without any grinding media, grinding seems to be another way to activate the hydration of slag using mechanical force.

2.2. Pore solution analysis

The pH of the pore fluid from the pastes mixed with NaOH solution was constant (Fig. 4), whereas that of the pastes mixed with DI water increased from 10.3 to 12 during 56 days of hydration with L/S = 0.45. With L/S > 3.0, the pH of the solution was slightly higher, and otherwise it established a similar trend. The concentration of alkali ions in the aqueous phase of each paste apparently controls the pH of the aqueous phase. The concentration of Na ions in the paste mixed with NaOH solutions was constant through 56 days of hydration. However, in the pastes mixed with DI water, it increased from 6.9 to 49.3 mmol when L/S = 0.45, and it increased from 2.84 to 16.5 mmol when L/S = 3.0. The addition of NaOH sets up a buffer in the pore fluids, but the pH of the pastes mixed with DI water is controlled by the dissolution of Ca and alkali ions from the solid.

The concentrations of Si, Al, Ca, and Mg in pore solution of each paste as a function of hydration time is shown in Fig. 5. For better understanding, the concentrations also are plotted against the pH of the fluid in Fig. 6. The concentration of Si and Al increased with the pH, whereas those of Ca and Mg decreased. This relationship between the pH and the ionic concentration of these species can be explained using the equilibrium solubility product, which depends on the Gibbs free energy of dissolution. For example, the solubility of Si in the aqueous solution is controlled by the standard free energy, ΔG°, and the thermodynamic equilibrium constant, K, of different silicate ions as given in Table 1. The reactions described in Table 1 also are shown in Fig. 7. Assuming the activity of $SiO_{2\,(quartz)}$ is 1, the activity of H_2SiO_3 in aqueous solution, $a_{(H_2SiO_3)}$ becomes a constant, and the activity of $HSiO_3^-$ ion, $a_{(HSiO_3^-)}$, is determined by pH and $a_{(H_2SiO_3)}$. Using the standard free energy, $\Delta G^\circ = -RT\ln K$, $a_{(HSiO_3^-)}$ becomes equivalent with $a_{(H_2SiO_3)}$ at pH 10 and linearly increases with the pH. Thus, even vitreous silica becomes unstable at pH 10 when $HSiO_3^-$ is thermodynamically favored over H_2SiO_3. When the same calculation is repeated for Ca, the activity of Ca^{2+}, $a_{(Ca^{2+})}$, decreases with the pH, whereas the activity of $Ca(OH)_2$, $a_{(Ca(OH)_2)}$, is a constant. The decrease in the concentration of Ca in highly alkaline solution is because $Ca(OH)_2$ is the thermodynamically favored species rather than Ca^{2+} ion when pH is higher than 11.5. This thermodynamic prediction has been verified for alkaline-lime-silicate glasses [38,39].

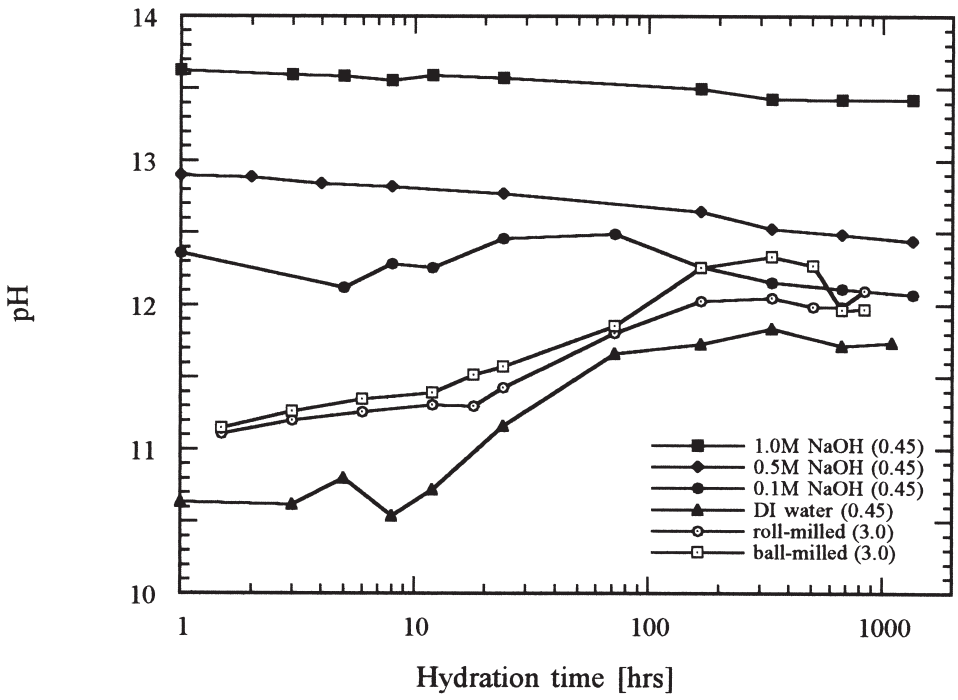

Fig. 4. The pH of pore fluids of GGBFS pastes as a function of hydration time.

However, all these calculations used the standard thermodynamic data taken at 25°C for crystalline phases. GGBFS is not a crystalline material and, therefore, has a different standard free energy of formation from pure silica or quartz. The Gibbs free energy of formation for an amorphous phase is usually higher than that for a crystalline phase, and this difference affects both solid and aqueous phases. Although this changes the absolute magnitude of the activities, it does not change the trend with respect to pH. As seen in Figs. 6A and 6B, the aqueous concentrations of Si and Ca in pore fluids show the same trend as do their activities. In our study, the concentration of Si started to increase around pH = 11.5, whereas the values from thermodynamic calculation show pH = 10. The decrease in the solubility of Ca with pH can be explained similarly by considering the reactions involving Ca ions, as shown in Table 1. At pH > 11.5, the Ca

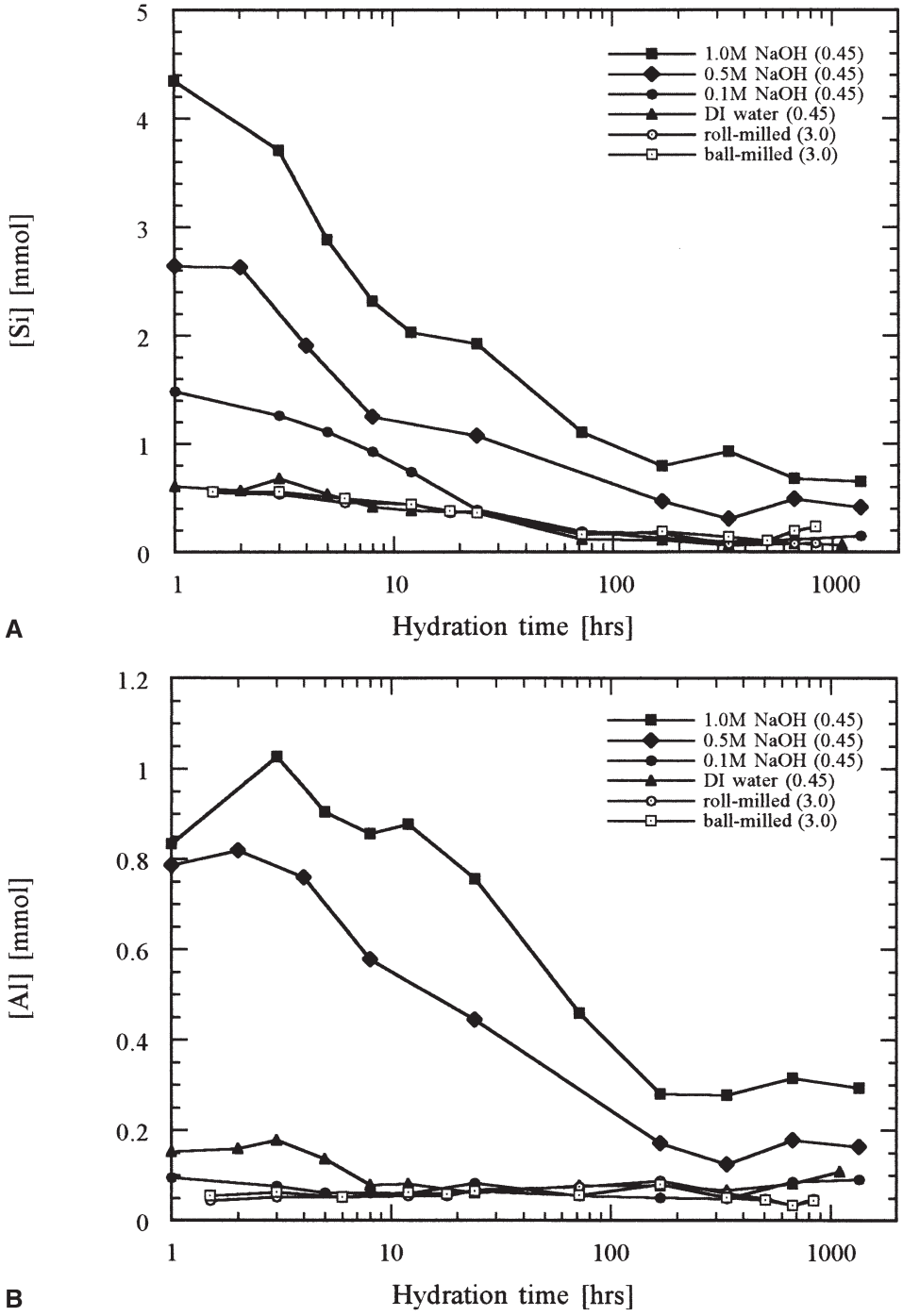

Fig. 5. Concentration of major components of GGBFS in pore fluids as a function of hydration time *(A)* Si, *(B)* Al, *(C)* Ca, and *(D)* Mg.

ion concentration drops, because the solid phase is thermodynamically favored; that is, the low concentration of Ca in this region is due to the lower equilibrium solubility of Ca^{2+} in a highly alkaline solution. The pH-dependent solubility of Si seems to be the most important factor explaining the alkali activation of GGBFS thermodynamically.

The relationship between pH and the solubility of Al and Mg also is seen in Figs. 6B and 6D. The concentration of Al in the pastes mixed with 0.4M and 0.1M NaOH varies greatly. The concentration of Mg was very low in all samples except the early age of GGBFS mixed with DI water. Thus, the amount of Al and Mg incorporated into the C-S-H should depend on the pH of solution. X-ray microanalysis by Wang and Scrivener [37] showed the ratios of Mg/Ca and Al/Ca in C-S-H were different in slag activated with either NaOH or Na_2SiO_3 (they showed very high concentrations of Si in pore fluids) after 1 day of hydration, but the ratios were not different for slag hydrated for 1 year.

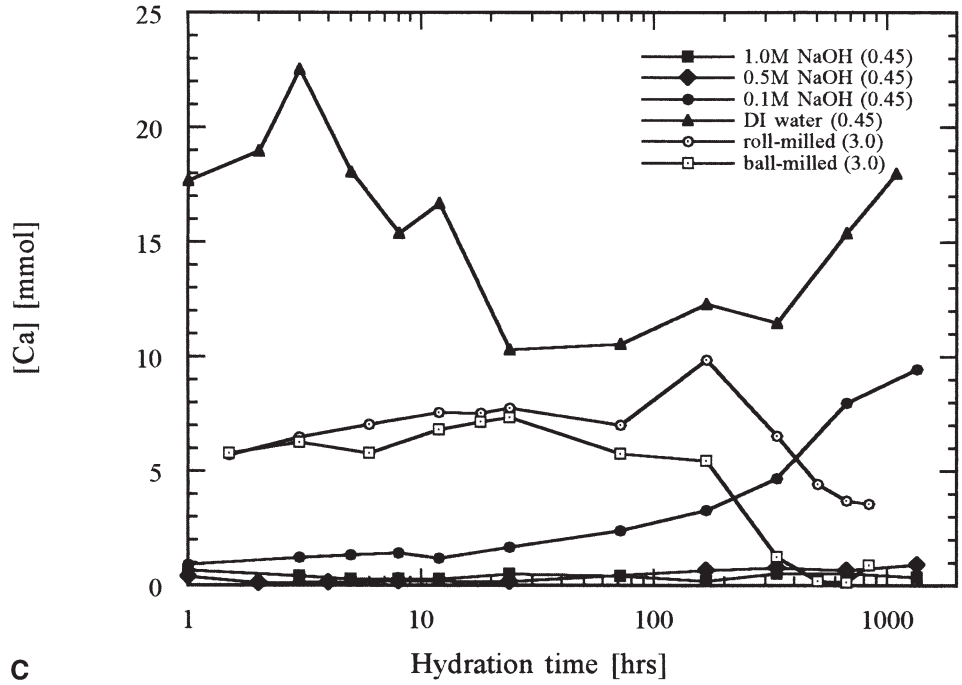

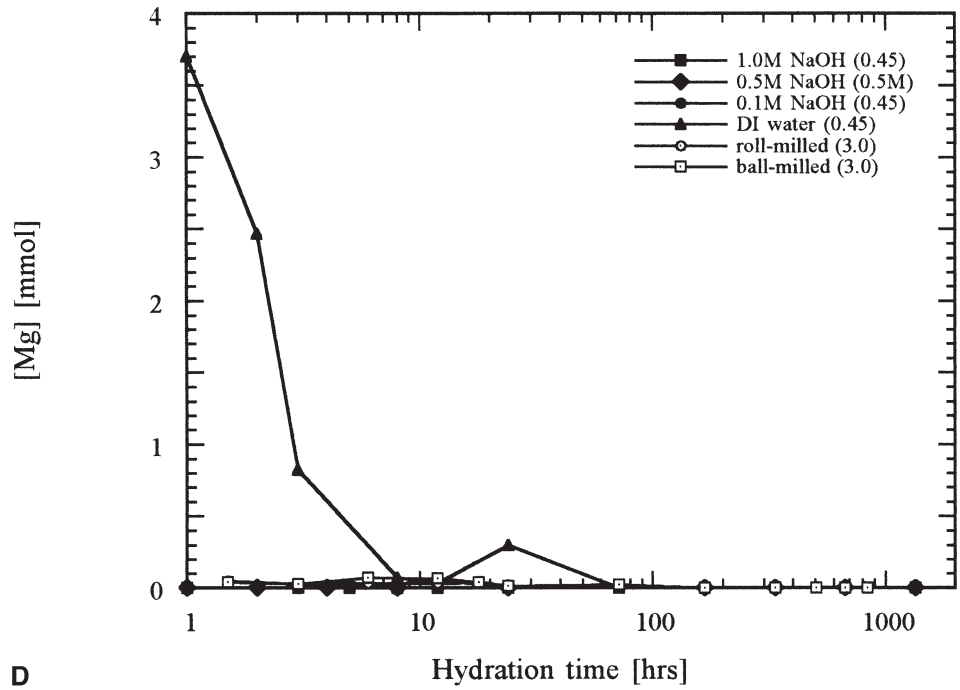

Fig. 5. (*continued*).

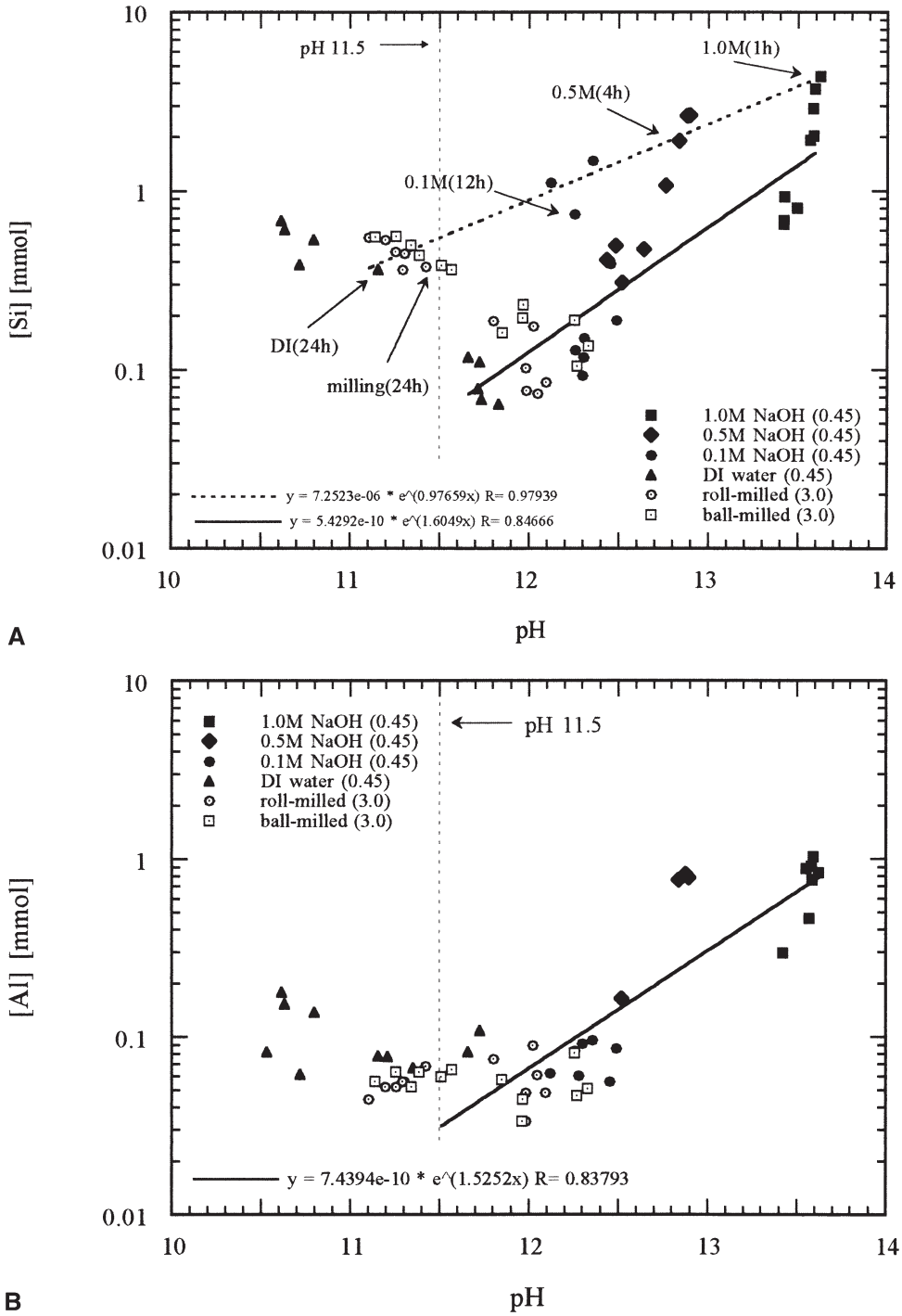

Fig. 6. Concentration of major components of GGBFS in pore fluids as a function of pH in pore fluids *(A)* Si, *(B)* A1, *(C)* Ca, and *(D)* Mg.

In Fig. 6A, the data suggest the existence of two separate lines above pH 11.5. Considering the age of the pastes and the results from XRD, the line with a higher Si concentration is associated with the fresh pastes before or during the very early stage of C-S-H formation. The data on the line with a lower Si concentration are from the later stage of hydration. When C-S-H forms in the paste, the thermodynamic equilibrium described in Table 1 must be changed to include the new solid, C-S-H, which is in contact with the aqueous phase; the solubility of Si should be determined by C-S-H, pH, and the solubility of Ca in pore fluid.

In Fig. 8, the Si concentration is plotted against the Ca concentration and superimposed on the water-rich region of the $CaO\text{-}SiO_2\text{-}H_2O$ phase diagram of two types of C-S-H [40]. The solubility of C-S-H formed in NaOH solutions resides on curve S, but C-S-H formed in DI water is on curve

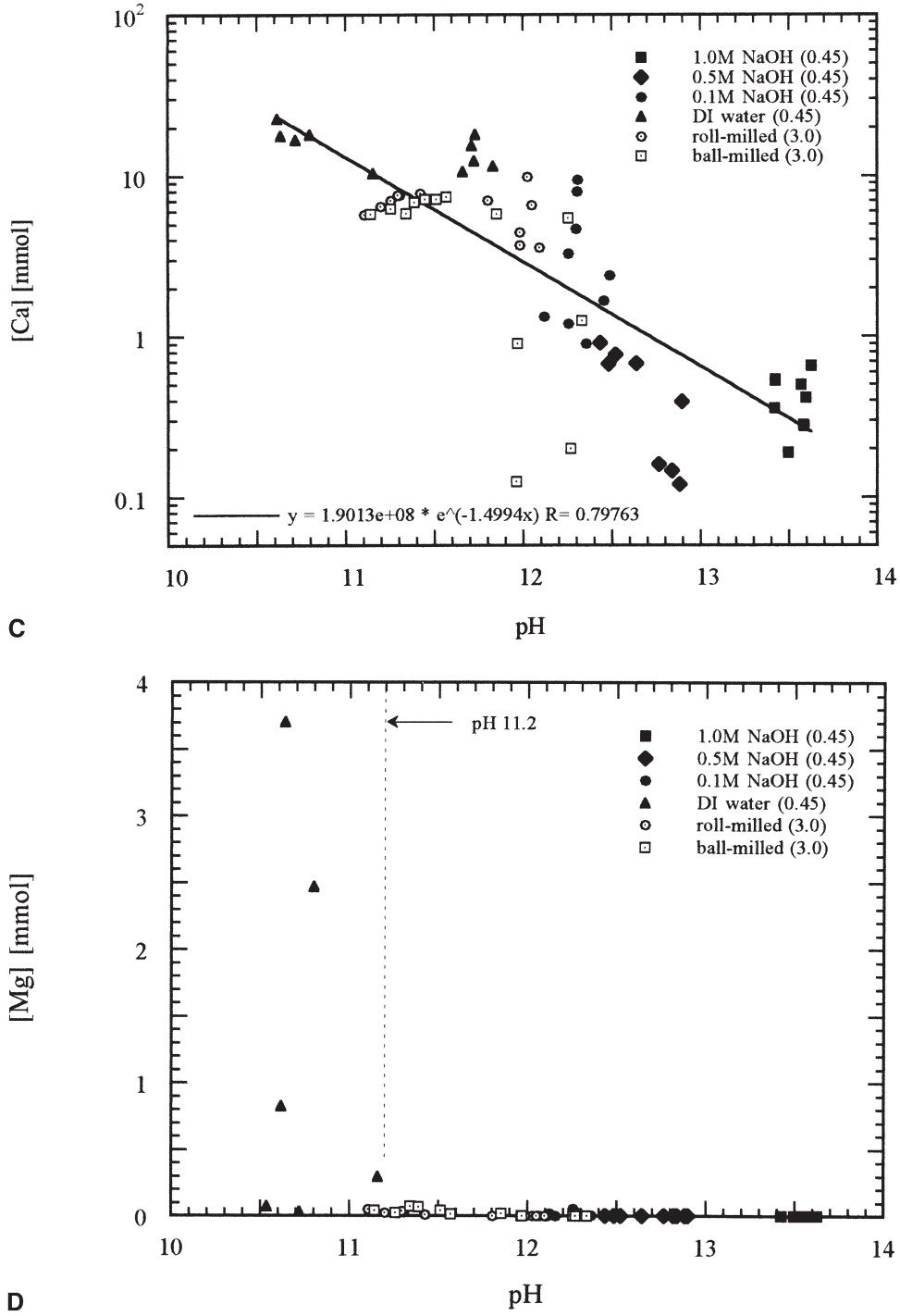

Fig. 6. (*continued*).

M. The solubility of Si and Ca in the pastes with L/S = 3.0 stayed very close to curve M during 1 day of milling with steel balls, then moved toward curve S. It took more than 7 days for the paste without steel balls to move away from curve M to curve S. The equilibrium state of C-S-H in the GGBFS pastes appears to be dependent on pH. Considering the pH at each data point, the solubility of Si and Ca stays very close to curve S with pH > 12 and close to curve M with pH < 12. The solubility of Si and Ca changes with the pH, and it may lead to the formation of C-S-H of a different nature. The paste mixed with 0.1M NaOH shows the solubility of Ca and Si is close to curve S until 14 days of hydration, but the solubilities got very close to curve M after 28 and 56 days of hydration as the pH of the solution decreases below pH 12. Considering the pH of the pastes mixed with DI water and the paste with 0.1M NaOH after 14 days of hy-

Table 1
Standard free energy and thermodynamic equilibrium constants of different ions in aqueous solution at 25°C [39]

Reaction	ΔG° (kcal/mol)	log K*
$SiO_{2(quartz)} + H_2O = H_2SiO_{3(aq)}$	7.1	$-5.20 = \log a(H_2SiO_3)$
$H_2SiO_{3(aq)} = HSiO_3^-{}_{(aq)} + H^+$	13.6	$-15.2 = \log a(HSiO_3^-) - pH$
$H_2SiO_{3(aq)} = SiO_3^{2-}{}_{(aq)} + 2H^+$	30.0	$-27.2 = \log a(SiO_3^{2-}) - 2pH$
$CaO + H_2O = Ca(OH)_{2\,(aq)}$	−6.28	$4.6 = \log a(Ca(OH)_2)$
$Ca(OH)_{2\,(aq)} + 2H^+ = Ca^{2+}{}_{(aq)} + 2H_2O$	−31.3	$27.6 = \log a(Ca^{2+}) + 2pH$

* $\ln K = -\Delta G°/RT = 2.303 \log K$.

dration, the pH of pore fluids appears to be a very important variable in controlling the ionic solubilities and the equilibrium between the aqueous phase and the surface solid phase.

McCurdy and Stein [17] reported that, during suspension hydration of C_3S, an equilibrium is established at pH 11.5 between one of the C-S-H gels and the solution, and they suggested that the hydration of C_3S is retarded under the circumstance of pH 11.5. It is very evident through this study that GGBFS in a solution with a pH below 11.5 has a solubility close to curve M in Fig. 8. Without activation aid, further hydration is hard to achieve. It has been suggested that a high pH solution activates the hydration of slag by solubilizing the water-impermeable layer on the surface of the slag particles [3]. This study also suggests the pH of the mixing solution may affect the thermodynamic nature of C-S-H by controlling the solubility of each component. Several studies [4,5,33] showed that increasing the slag content in OPC pastes reduces the C/S ratio and progressively changes the morphology of the C-S-H. The more slag in the OPC paste, the lower the C/S ratio of C-S-H, and the C-S-H of a low C/S has a foil-like morphology compared to the fiberlike C-S-H of a high C/S ratio. Richardson et al. [41] also pointed out that GGBFS pastes showed a foil-like morphology whether mixed with 5M KOH or just water. The relationship between the morphology of C-S-H and the macroscopic properties of pastes needs more investigation.

3. Conclusion

The solubilities of Si, Ca, Al, and Mg are strong functions of the pH. High pH increases the concentration of Si and Al, but reduces that of Ca and Mg in the pore fluids. This pH-dependent behavior was well explained using thermodynamic functions such as standard free energy and equilibrium constants of each species.

The pH-dependent solubilities also explain why the pH of the mixing solution must be higher than pH 11.5 to effectively activate the hydration of GGBFS. At a pH lower than 11.5, the equilibrium solubility of silica is low, and GGBFS simply does not dissolve.

The pH of the mixing solution is expected to have a significant effect on the nature of C-S-H by affecting the chemistry of the pore solutions. A high pH in the pore fluids may help the formation of C-S-H of a low C/S ratio and/or a different physical distribution because of the solubility of silica. Hydrotalcite seems to be a phase that should form when a high degree of hydration is reached in GGBFS pastes, whereas the C-S-H of a relatively low C/S ratio may be the main hydration product of alkali-activated GGBFS.

Acknowledgments

This work was funded by the U.S. Department of Energy (Grant DE-FG02-91ER45460) and the NSF Center for the Science and Technology of Advanced Cement Based Materials (Grant CHE-9120002). Their financial support is gratefully acknowledged.

References

[1] ACI Committee 226, Ground Granulated Blast Furnace Slag as a Cementitious Constituent in Concrete, ACI manual of Concrete Practice, 226.1R., 1989 pp 1–16.
[2] H. Uchigawa, 8th International Congress on the Chemistry of Cement, Rio de Janeiro, Vol. 3, 1986, pp. 249–280.
[3] P. K. Mehta, 3rd International Conference on Fly Ash, Silica Fume, and Natural Pozzolans in Concrete, Tronheim, Norway, 1989, pp. 1–43.
[4] T. Hakkinen, Cem Concr Res 23 (1993) 407–421.
[5] T. Hakkinen, Cem Concr Res 23 (1993) 518–530.
[6] M. Regourd, J.H. Thomassin, P. Ballif, J.C. Touray, Cem Concr Res 13 (1983) 549–556 (1983).
[7] S.A. Greenberg, T.N. Chang, J Phys Chem 69 (1965) 182–188.
[8] H.M. Jennings, The developing microstructure in Portland cement, in: S.N. Ghosh (Ed.), Advances in Cement Technology, Pergamon Press, New York, 1983, pp. 349–396.
[9] H.F.W. Taylor, et al., RILEM Committee 68-MMH, Task Group 3, Mater Const (Paris) 17 (1984) 457–468.
[10] S.A. Greenberg, E.W.J. Price, Phys Chem 61 (1957)1539–1541.
[11] G.B. Alexander, W.M. Heston, R.K. Iler, J Phys Chem 58 (1954) 453–455.
[12] S.A. Greenberg, J Phys Chem 61 (1957) 196–197.
[13] K. Andersson, B. Allard, M. Bengtsson, B. Magnusson, Cem Concr Res 19 (1989) 327–332.
[14] E.P. Flint, L.S. Wells, Bureau Standards J Res 12 (1934) 751–783.
[15] P.S. Roller, E.J. Ervin Jr, J Am Chem Soc 62 (1940) 461–471.
[16] S.A. Greenberg, T.N. Chang, E. Anderson, J Phys Chem 64 (1960) 1151–1157.
[17] K.G. McCurdy, H.N. Stein, Cem Concr Res 3 (1973) 247–262.
[18] K.G. McCurdy, H.N. Stein, Cem Concr Res 3 (1973) 509–520.
[19] A.R. Ramanchandran, M.W. Grutzeck, J Am Ceram Soc 76 (193) 72–80.
[20] G.L. Kalousek, J Res National Bureau Standards 32 (1944) 285–302.
[21] K. Suzuki, T. Nishikawa, H. Ikenaga, S. Ito, Cem Concr Res 16 (1986) 333–340.
[22] K. Suzuki, T. Nishikawa, S. Ito, Cem Concr Res 15 (1985) 213–224.
[23] D.E. Macphee, K. Luke, F.P. Glasser, E.E. Lachowski, J Am Ceram Soc 72 (1989) 646–654.
[24] H.F.W. Taylor, J Chem Soc Lond 4 (1950) 3682–3695.
[25] I.G. Richardson, G.W. Groves, Cem Concr Res 23 (1993) 131–138.
[26] M. Kersten, Environ Sci Technol 30 (1996) 2286–2293.
[27] E.M. Gartner, H.M. Jennings, J Am Ceram Soc 70 (1987) 743–749.
[28] S. Goto, K. Akazawa, M. Daimon, Cem Concr Res 22 (1992) 1216–1223.

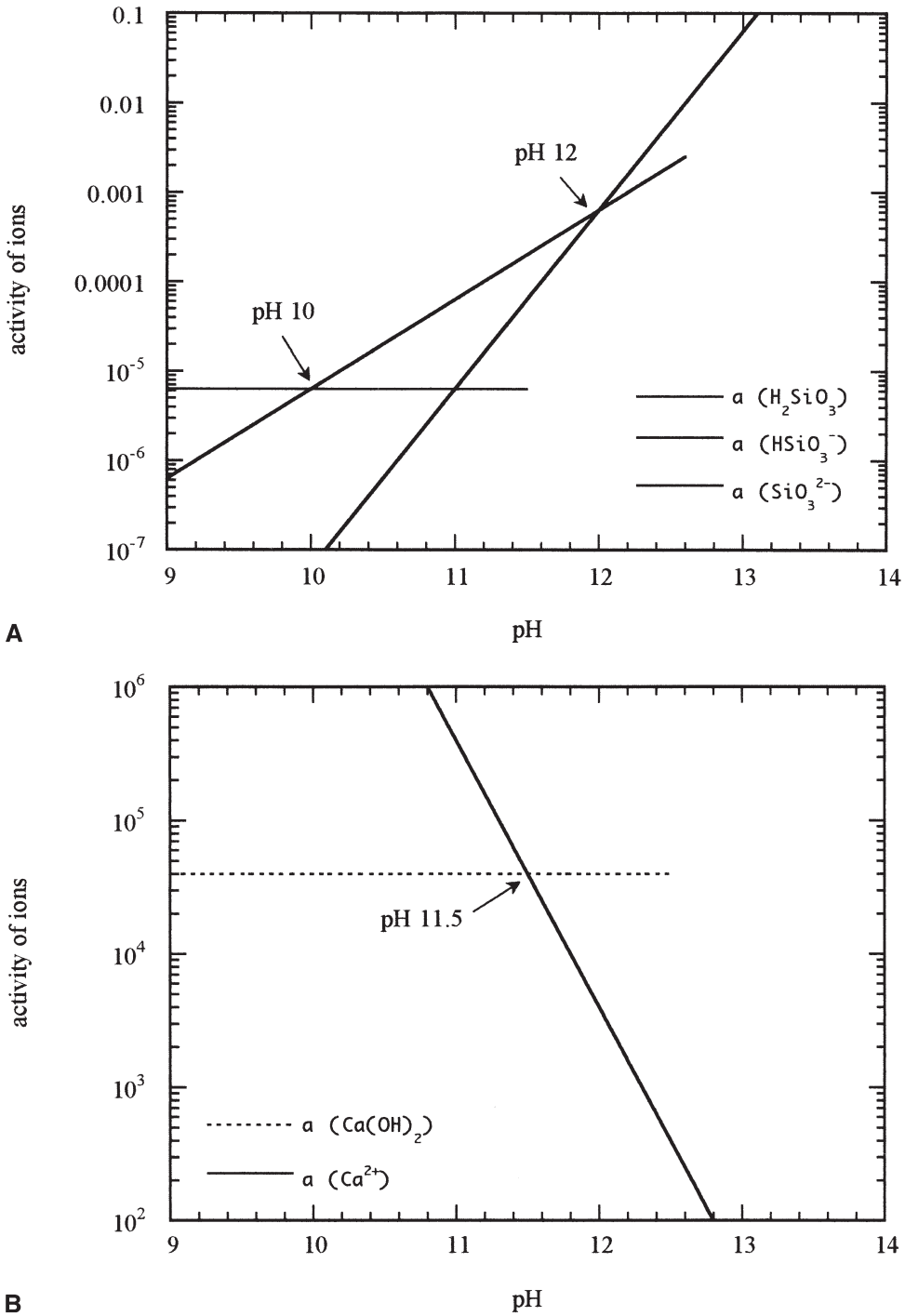

Fig. 7. Thermodynamically calculated activity of aqueous ions of *(A)* Si and *(B)* Ca as a function of pH.

[29] B.J. Christensen, Microstructure Studies of Hydrating Portland CementBased Materials Using Impedance Spectroscopy, Northwestern University, Evanston, IL, Ph.D. Thesis, 1993, pp. 103–115.
[30] B.J. Christensen, R.T. Coverdale, R.A. Olson, S.J. Ford, E.J. Garboczi, H.M. Jennings, T.O. Mason, J Am Ceram Soc 77 (1994) 2789–2802.
[31] R.S. Barneyback, S. Diamond, Cem Concr Res 11 (1981) 279–285.
[32] M.C. Gastuche, G. Brown, M.M. Nortland, Clay Minerals 7 (1967) 177–192.
[33] I.G. Richardson, G.W. Groves, J Mater Sci 27 (1992) 6204–6212.
[34] H.F.W. Taylor, Cement Chemistry, Academic Press, London, 1990.
[35] H.F.W. Taylor, Adv Cem Based Mater 1 (1993) 38–46.
[36] A.M. Harrison, N.B. Winter, H.F.W. Taylor, MRS Symp Proc 86 (1986) 199–208.
[37] S.D. Wang, K. Scrivener, Cem Concr Res 25 (1995) 561–571.
[38] T.M. ElShamy, J. Lewins, R.W. Douglas, Glass Technol 13 (1972) 81–87.
[39] A. Paul, Chemistry of Glasses, Chapman and Hall, London, 1982.
[40] H.M. Jennings, J Am Ceram Soc 69 (1986) 614–618.
[41] I.G. Richardson, A.R. Brough, G.W. Groves, C.M. Dobson, Cem Concr Res 24 (1994) 813–829.

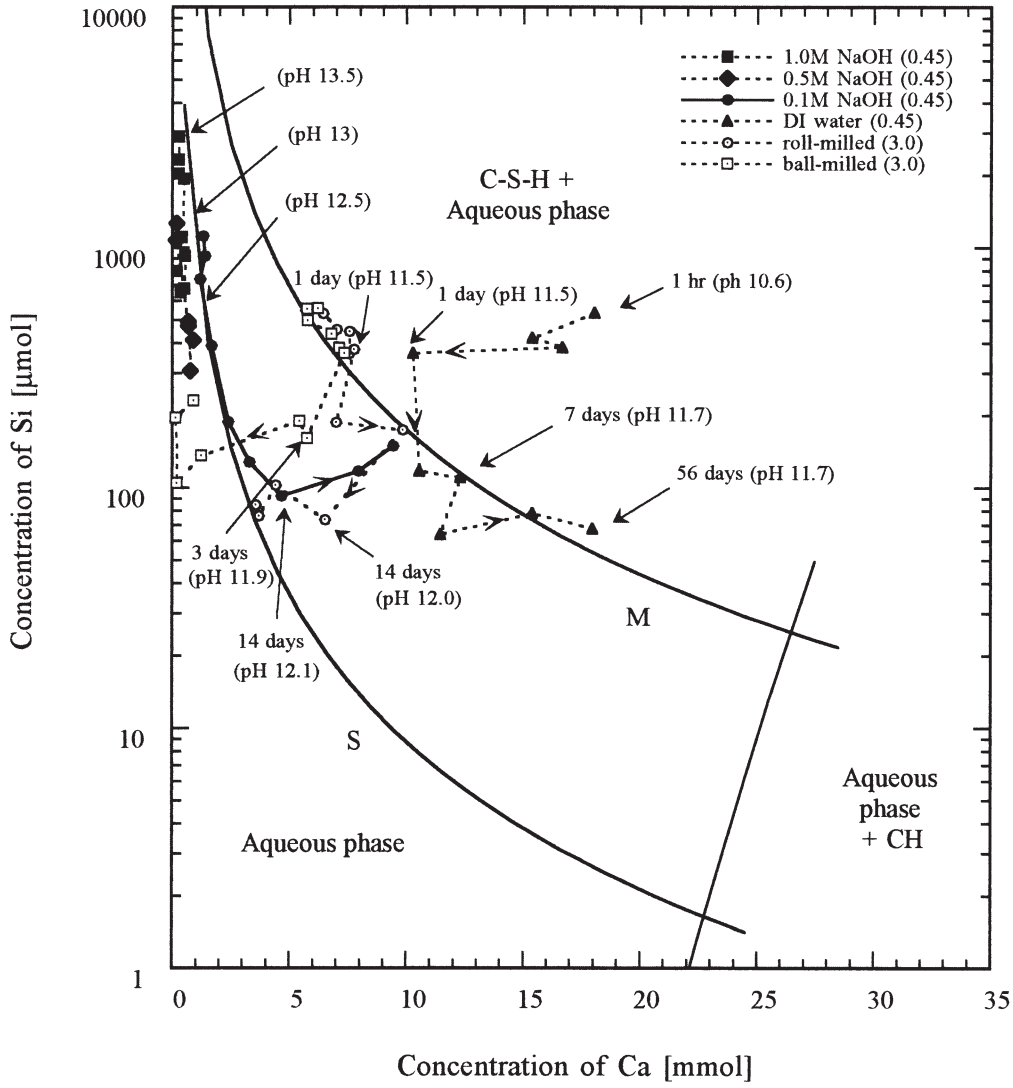

Fig. 8. Concentration of Si and Ca on the water-rich region of the $CaO\text{-}SiO_2\text{-}H_2O$ phase diagram.